

Observation of $h/2e$ resistance oscillation, double resistance anomalies, and excessive resistance in mesoscopic $\text{Au}_{0.7}\text{In}_{0.3}$ rings

H. Wang, M. M. Rosario, H. L. Russell, and Y. Liu

Department of Physics, The Pennsylvania State University, University Park, PA 16802

(Dated: February 8, 2020)

We report the observation of $h/2e$ resistance oscillation, double resistance anomalies near the superconducting transition, and a magnetic-field-induced, low-temperature metallic state with an excessive resistance in a magnetic field in mesoscopic $\text{Au}_{0.7}\text{In}_{0.3}$ rings. We show that the observed phenomena can be qualitatively explained in the picture of charge imbalance near the normal metal-superconductor (N-S) interface. We also discuss the nature of the metallic state with an excessive resistance.

PACS numbers: 74.78.-w, 74.81.-g, 74.40.+k

I. INTRODUCTION

Recent structural and electrical transport studies of $\text{Au}_{0.7}\text{In}_{0.3}$ films have shown that this material represents a novel system for studying the disorder effects on superconductivity in two dimension (2D). These films can be modeled as a 2D array of superconductor-normal metal-superconductor (SNS) Josephson junctions¹, with both the local gap and Josephson coupling of the junctions varying randomly. Conventional granular films, such as those prepared by quench deposition, on the other hand, are modeled as a random array of superconductor-insulator-superconductor (SIS) Josephson junctions. The phase of the superconducting order parameter, ϕ , and the number of Cooper pairs, N , are conjugate variables quantum-mechanically, and are subject to an uncertainty relation. Therefore, the confinement of Cooper pairs in SIS granular films due to charging energy leads to the phase fluctuation, and a 2D superconductor-to-insulator transition (SIT) if the phase fluctuation is sufficiently strong. Cooper pairs in $\text{Au}_{0.7}\text{In}_{0.3}$ films, however, are not subject to similar spatial confinement, even though these films are still strongly disordered because of the spatially varying amplitude of the superconducting order parameter.

Interesting physical phenomena have been found in planar and cylindrical films of $\text{Au}_{0.7}\text{In}_{0.3}$ ^{2,3,7}. In particular, because of the superconducting fluctuations, the amplitude of the magnetic fingerprints just above T_c was found to be greatly enhanced², as anticipated⁴. An $h/4e$, rather than $h/2e$, resistance oscillation, was also found³. While the physical origin of the observed $h/4e$ resistance oscillation is not understood, it was proposed that it might be associated with the presence of π -junctions between adjacent In-rich grains that would possess a negative rather than positive Josephson coupling constant. The presence of these random distributed π -junctions leads to new minima in the free energy of the cylinder that can be viewed as an ensemble of individual $\text{Au}_{0.7}\text{In}_{0.3}$ rings. The resistance oscillation follows the landscape of the free energy and has an unconventional $h/4e$ period.

The interesting question is whether a similar $h/4e$ resistance oscillation also exists in mesoscopic rings of $\text{Au}_{0.7}\text{In}_{0.3}$. In the π -junction scenario described above, the resistance oscillation of a cylinder is $h/4e$ because of the ensemble average. For a single ring, the resistance oscillation would incur a phase shift by π for the odd number of π -junctions and no phase shift for even number of π -junctions. However, the oscillation would still be of $h/2e$ period.

Another interesting phenomenon characteristic of the mesoscopic superconducting structures is the resistance anomaly.¹⁰ This phenomenon features a resistance peak higher than the normal-state value R_N at the onset of the superconducting transition $R(T)$. Considerable studies on this unusual phenomenon^{11,12,13,14,15,16} have led to the understanding that the resistance anomaly is related to the charge imbalance near the normal metal-superconductor (N-S) interface. Such a N-S interface in mesoscopic structures can result from the sample inhomogeneity and/or phase slip centers (PSC's) formed at the weakest spots in the sample. Contrary to the equilibrium state of the superconducting condensate where quasiparticles and Cooper pairs share the same electrochemical potential value, the carrier injection at a N-S interface leads to a difference between the chemical potential of the Cooper pairs (μ_p) and that of quasiparticles (μ_q), a phenomenon commonly referred to as charge imbalance. The spatial variations of μ_p and μ_q lead to the observed resistance anomaly.

$\text{Au}_{0.7}\text{In}_{0.3}$, consisting of In-rich grains that first become superconducting right below their onset T_c 's, may represent a rather unique system for the study of resistance anomaly. It has been suggested that the shape of the N-S interface has significant effect in determining the magnitude of the resistance anomaly.^{12,15} Thus it is natural to conjecture that the presence of irregularly shaped In-rich grains in $\text{Au}_{0.7}\text{In}_{0.3}$ might lead to new features in resistance anomaly.

In this paper, we report our experimental results from electrical transport measurements of mesoscopic $\text{Au}_{0.7}\text{In}_{0.3}$ rings prepared by e-beam lithography. No $h/4e$ period was observed, as expected. Whether there was a phase shift by π in the $h/2e$ oscillation, however,

could not be determined because of the experimental limitations. Most interestingly, we observed double resistance anomalies in these rings and a magnetic-field-induced metallic state with an excessive resistance in the intermediate magnetic field range at low temperatures. The metallic state appears to be a consequence of the amplitude fluctuation in the order parameter.

II. SAMPLE PREPARATION AND MEASUREMENTS

Conventional e-beam lithography was used to prepare the $\text{Au}_{0.7}\text{In}_{0.3}$ rings. The ring patterns were generated using double-layer PMMA/MMA resist on either Si wafer coated with a 200Å-thick SiO_2 layer or polished 1cm×1cm sapphire substrate. Sequential thermal evaporation of alternating 99.9999% pure Au and In layers, with the layer thickness determined by the desired atomic ratio of Au to In, was carried out at ambient temperature in a conventional evaporator with a vacuum of 1×10^{-6} torr or slightly better. The ring pattern was placed with respect to the Au and In sources so as to minimize the shadow effects during evaporation. After the liftoff, atomic force microscope (AFM) was used to image the resulted $\text{Au}_{0.7}\text{In}_{0.3}$ rings before the measurement leads were attached.

Five rings with diameters either 0.75μm or 1μm and a thickness of 35 nm were measured. An AFM image of a 1-μm-diam ring is shown in Fig. 1a, with its schematic shown in Fig. 1b for a detailed illustration of sample geometry. The 0.75-μm-diam rings have a similar configuration with a 4 μm voltage-probe separation.

Electrical transport measurements were carried out in a dilution refrigerator with a base temperature $<20\text{mK}$ and a superconducting magnet. All electrical leads entering the cryostat were filtered by RF filters with an attenuation of 10dB at 10MHz and 50dB at 300MHz. Resistance characteristics were measured with a d.c. current source and a nanovoltmeter. The magnetic field was applied perpendicular to the substrate.

In Fig. 2, resistance as function of temperature at zero magnetic field is shown for all five rings. The structural and electrical parameters are listed in Table I. The typical values for resistivity, ρ , are about 3 times larger than that for $\text{Au}_{0.7}\text{In}_{0.3}$ films with the same thickness¹. The values of T_c , evaluated at the $0.01R_N$ levels, are significantly lower than those of films except for Ring 6-075.

These rings appear to belong to two groups, based on the values of T_c and features in $R(T)$ superconducting transition. Ring 6-075, which has a significant higher T_c and a conventional resistive transition, appears to be a homogeneous ring. The rest samples, on the other hand, have low T_c 's and show additional features near the transition-double resistance peaks. These rings clearly have higher degree of disorder, thus belonging to inhomogeneous rings. However, the resistivities for both homogeneous and inhomogeneous rings are not significantly

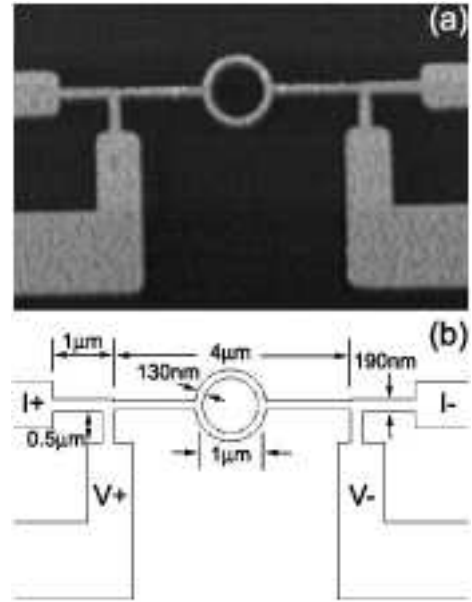


FIG. 1: a) Atomic force microscope (AFM) image of a 1-μm-diam $\text{Au}_{0.7}\text{In}_{0.3}$ ring. b) A schematic of the ring specifying all relevant dimensions. The 0.75-μm-diam rings have a similar configuration with a 4 μm voltage-probe separation.

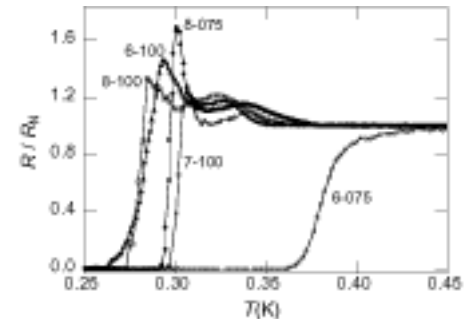


FIG. 2: Normalized resistances as function of temperature $R(T)$ for five $\text{Au}_{0.7}\text{In}_{0.3}$ rings. Rings are labeled as indicated. Parameters for these rings are shown in Table I.

different.

III. h/2e OSCILLATION

For the homogeneous Ring 6-075, a $h/2e$ resistance oscillation with large amplitude was observed in the transition regime (Fig. 3b). The physical origin of the $h/2e$ resistance oscillation is that the free energy of a doubly-connected superconductor is a periodic function of the flux threading the superconductor with a period of $h/2e$, the flux quanta. For the inhomogeneous rings, a weak $h/2e$ resistance oscillation was observed from near the transition temperatures (Fig. 4b) down to the base temperature ≈ 20 mK. The amplitude of the oscillation, $\Delta G = \Delta(1/R_\square)$, is around $0.5e^2/h$, much smaller than

TABLE I: The structural and electrical parameters of the rings. T_c is evaluated at the $0.01R_N$ level.

Sample diameter (μm)	R_N (Ω)	$R_{N,\square}$ (Ω)	ρ ($\mu\Omega\text{ cm}$)	T_c (K)
6-075	0.75	520	13.5	40.6
6-100	1.00	510	13.5	40.4
7-100	1.00	472	12.5	37.4
8-075	0.75	433	11.3	33.8
8-100	1.00	469	12.4	37.2

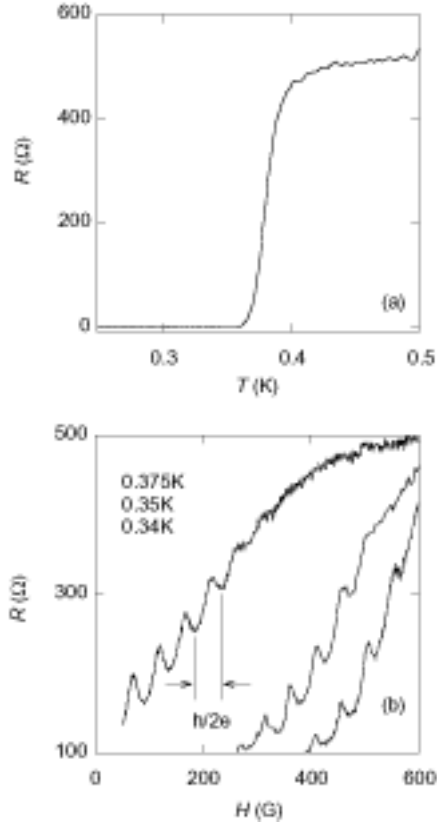


FIG. 3: a) $R(T)$ of Ring 6-075 at zero magnetic field; b) Magnetoresistance oscillations of Ring 6-075 at various temperatures as indicated. The period of resistance oscillations in b) is $h/2e$.

that observed in Ring 6-075. As a result, this oscillation should be identified as the consequence of coherent backscattering of normal electrons in disordered systems, a weak localization phenomenon. Resistance oscillation resulting from this process has a period of $h/2e$, also known as the Sharvin-Sharvin oscillation¹⁷. The associated negative magnetoresistance background shown in Fig. 4b is related to charge imbalance and will be addressed in the next section.

In a previous study of $\text{Au}_{0.7}\text{In}_{0.3}$ cylinders, a resistance oscillation of $h/4e$ was found at the low-temperature part of the resistive transition along with the conventional $h/2e$ resistance oscillation.³ As mentioned earlier, the

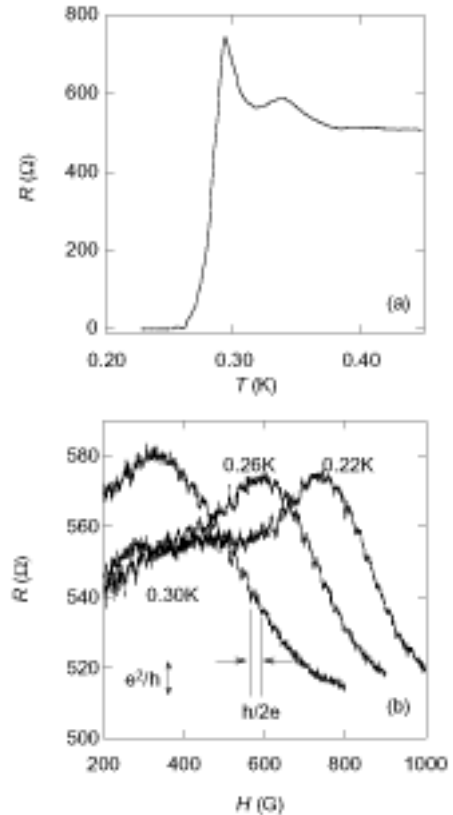


FIG. 4: a) $R(T)$ of Ring 6-100 at zero magnetic field; b) Magnetoresistance oscillations of Ring 6-100 at various temperatures as indicated. The period of resistance oscillations in b) is $h/2e$.

resistance close to the superconducting state tracks the free energy landscape of the superconductor. The observation of an additional $h/4e$ resistance oscillation at the low-temperature limit therefore signaled the emergence of additional minima in the free energy.³ These additional minima were proposed to be originated from the presence of the so-called π -junctions as well as the conventional 0-junctions. These junctions are formed by the In-rich grains embedded in $\text{Au}_{0.9}\text{In}_{0.1}$ normal-metal matrix.¹ Because of the mesoscopic fluctuations in an applied field, some of the Josephson coupling constants between two adjacent In-rich grains are negative, giving rise to the existence of π -junctions.³

The presence of π -junctions in a cylinder will lead to the presence of additional minima in free energy at $\Phi = n\Phi_0/2$, where n is an odd number. In a given magnetic field, there will be an induced circulating current distribution going through a number of junctions. The distribution of the currents will be such that the free energy is minimized. To visualize this, a collection of loops of circulation current such that the fluxoid $\Phi' = \Phi_{\text{ext}} + \sum_i \Phi_i$ is quantized for each loop is illustrated in Fig. 5a, where Φ_{ext} is the applied magnetic flux and Φ_i is the phase change of the superconducting order parameter across the junction i along the loop. Each loop

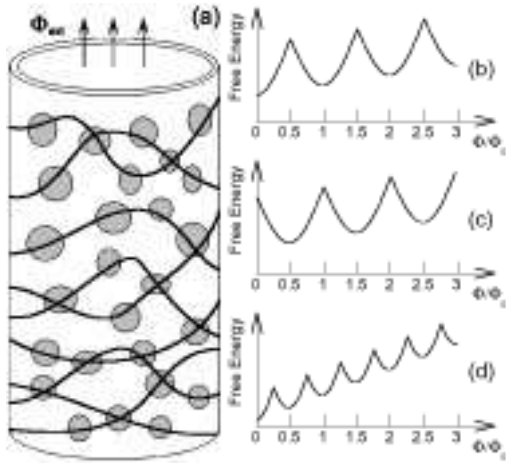


FIG. 5: Schematics of a) a possible distribution of current loops (curled solid lines on the cylindrical surface) in the cylinder; b) free energy for a loop with even-number of π -junctions; c) free energy for a loop with odd-number of π -junctions; d) free energy for a cylinder which can be modeled as a collection of loops. For a), gray circles are the In-rich grains which become superconducting at low temperatures. 0- or π junctions form through the coupling of these superconducting grains. Φ_{ext} is the applied magnetic flux threading the cylinder. For b) and c), the free energy is a periodic function of Φ , with a conventional period of $\Phi_0 = h/2e$. For d), the period is halved to become $h/4e$ as the flux is tuned. Redistribution of the circulation current as the magnetic field is varied is involved.

consists of either even or odd number of π -junctions. For the loops with even number of π -junctions, the free energy has minima at integer flux quanta (Fig. 5b) while for loops with odd number of junctions the minima in free energy are at half-integer flux quanta (Fig. 5c).³ At $\Phi_{\text{ext}} = m\Phi_0$, where m = integers, the current distribution will be such that as many loops with even number of π -junctions as possible will be present. At $\Phi_{\text{ext}} = n\Phi_0/2$, where n = odd numbers, on the other hand, the collection of current loops will redistribute so that as many loops with odd number of π -junctions as possible will be created. As a result, there will be minima in free energy at both integer and half-integer flux quanta (Fig. 5d), leading to $h/4e$ resistance oscillation.

For a ring such as that shown in Fig. 1, the width of the ring (130 nm) is comparable to the zero-temperature superconducting coherence length, ξ ($\approx 0.1\mu\text{m}$). Therefore, only one superconducting grain can form over the width of the ring at low temperatures. As a result, redistribution of current loop in the ring is not allowed. The number of π -junctions in the loop is fixed. The resistance oscillation will therefore be a conventional one if there are even number of π -junctions. However, if there are odd number of π -junctions, there will be a $\Phi_0/2$ shift in the resistance oscillation. Namely, the resistance oscillation will have its maxima rather than minima at integer flux quanta. Unfortunately, for all the rings that we fabri-

cated and measured, only Ring 6-075 turned out to be homogeneous. However, no evidence showed that resistance maxima exist at integer flux quanta for this ring. Consequently, we are unable to draw a definite conclusion on the existence of π -junctions in the $\text{Au}_{0.7}\text{In}_{0.3}$ rings based on the data we have.

IV. DOUBLE RESISTANCE ANOMALIES

A. Double resistance anomalies near the superconducting transition in $R(T)$

For inhomogeneous rings, a distinct feature in $R(T)$ curves taken in zero magnetic field (Fig. 2) is the presence of two resistance peaks near the superconducting transition. The lower-temperature resistance peak (LTRP) is relatively sharp, with a resistance about 30-70% higher than the normal-state resistance, R_N . The higher-temperature resistance peak (HTRP) with the onset temperature around 0.4K is broader and smaller in height (10-20%) than the LTRP.

The above phenomenon is referred to here as the double resistance anomalies in contrast to the resistance anomaly of single resistance peak observed previously in Al structures. As proposed originally by Santhanam¹⁰ and confirmed in various follow-up experiments^{11,12,13,14,15,16}, the anomaly in Al structures can be qualitatively understood in the framework of charge imbalance near a N-S interface. Such N-S interfaces occur in mesoscopic structures as a result of either sample inhomogeneity or spontaneously formed phase-slip centers (PSCs) near the superconducting transition. As to be described in more details below, the different spatial variations of electrochemical potentials of quasi-particles, Cooper pairs and extrapolated normal electrons on the superconducting side of the N-S interface result in the resistance anomaly.

B. Charge imbalance model

Charge imbalance is a nonequilibrium process generated by charge perturbations such as normal electron injection through the N-S interface. Consider now an 1D N-S interface at which the energy gap $\Delta = 0$ (Fig. 6). The gap Δ reaches the bulk value Δ_0 over the coherence length ξ . Close to T_c , the injection of normal current from the normal side (N) causes nonequilibrium distribution of quasiparticles on the superconducting side (S), which relaxes back to its equilibrium value over the charge imbalance length Λ_Q . The electroneutrality requires a corresponding decrease in the charge of the condensate to counter the increase of quasiparticle charge, thus leading to a spatial variation of chemical potential of quasi-particles, μ_q , and that of Cooper pairs, μ_p . In the normal side of the N-S interface, μ_n varies linearly spatially and matches with μ_q and μ_p at the interface¹⁹.

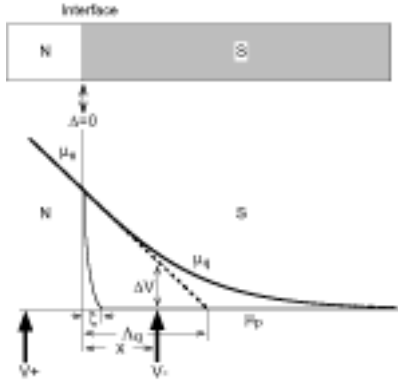


FIG. 6: Schematic of a charge imbalance model explaining resistance anomaly. μ_p , μ_q , and μ_n are the chemical potentials of Cooper pairs, quasiparticles in the superconductor (S), and normal electrons in the normal metal (N), respectively. ξ is the superconducting coherence length. Λ_Q the charge imbalance length. x is the distance between the voltage leads (V^-) and the interface where the gap $\Delta = 0$.

Inside the superconducting region, in the absence of any supercurrent (near T_c), μ_q can be approximated as²⁰

$$\mu_q(x) = -e\Lambda_Q \rho I \tanh(x/\Lambda_Q), \quad (1)$$

where ρ is the normal-state resistance per unit length, I is the current, and x is the distance from the N-S interface. Because the superconducting voltage leads probe μ_p , a potential difference between the extrapolated μ_n and the μ_p , ΔV (Fig. 6), gives rise to a resistance peak when the voltage leads are placed at $x < \Lambda_Q$ from the interface. The magnitude of this resistance rise is roughly given by

$$\Delta R(x) = (\Lambda_Q - x)\rho. \quad (2)$$

In previous experiments, a value on the order of 10 μm was typically quoted for Λ_Q in Al mesoscopic structures¹⁴. The values of physical parameters needed for estimating Λ_Q in $\text{Au}_{0.7}\text{In}_{0.3}$ are not available.¹ However, following the formulae in Ref. 21,

$$\Lambda_Q = \sqrt{D\tau_Q}, \quad (3)$$

where D is the electron diffusion coefficient and τ_Q the related relaxation time. At $T \approx T_c$,

$$\tau_Q = \frac{4}{\pi} \frac{k_B T_c}{\Delta(T)} \tau_E, \quad (4)$$

where $\tau_E \sim \frac{k_B T}{\hbar} \left(\frac{T}{\Theta_D} \right)^2$ is the inelastic relaxation time due to electron-phonon interaction and Θ_D the Debye temperature. Based on Eq. 3 and 4, Λ_Q for $\text{Au}_{0.7}\text{In}_{0.3}$ is expected to be significantly larger than our ring size because of the low T_c at which the anomalies occur.

Equation 4 is an approximation for τ_Q at $T \approx T_c$. A more rigorous theory taking into account various pair breaking mechanisms including magnetic field by Schmid and Schön²⁴ yields

$$\tau_Q = \frac{4k_B T}{\pi \Delta(T, B)} \sqrt{\frac{\tau_E}{2\Gamma}}, \quad (5)$$

and

$$\Gamma = \frac{1}{\tau_s} + \frac{1}{2\tau_E} + \frac{D}{2} \left(\frac{4m^2 v_s^2}{\hbar^2} - \frac{1}{\Delta} \frac{\partial^2 \Delta}{\partial x^2} \right). \quad (6)$$

τ_s is the scattering time related to orbital pair-breaking and spin-flipping process. Close to T_c and in the absence of paramagnetic impurities, τ_s is given by²⁵

$$\tau_s(T, B) = \frac{\hbar}{\Delta(T=0, B=0)} \frac{B_c(T=0)^2}{B^2}. \quad (7)$$

Therefore an increase of the magnetic field can decrease τ_s , and Λ_Q , leading to the suppression of resistance anomaly.

C. Two-stage charge imbalance model

Below we present a two-stage charge imbalance model to explain the double resistance anomalies observed in our $\text{Au}_{0.7}\text{In}_{0.3}$ rings. This model, based on the SNS structural characteristic of $\text{Au}_{0.7}\text{In}_{0.3}$ and the specific sample geometry and morphology, can qualitatively explain the main features of the double resistance anomalies observed in the $\text{Au}_{0.7}\text{In}_{0.3}$ rings.

In this picture, the double resistance anomalies result from the growth of superconducting regions in size, d , in comparision with the charge imbalance length, Λ_Q , in our particular sample geometry as the temperature is lowered. HTRP corresponds to the regime in which the size of the superconducting regions $d < \Lambda_Q$ and LTRP corresponds to that in which $d > \Lambda_Q$.

$\text{Au}_{0.7}\text{In}_{0.3}$ is composed of In-rich grains embedded in the normal-metal matrix $\text{Au}_{0.9}\text{In}_{0.1}$. These In-rich grains will grow in size and join neighboring grains to form a larger superconducting region, with a typical size d , when temperature is first lowered to below their onset T_c 's. The distribution of these superconducting regions in the sample at this temperature is illustrated in Fig. 7a. The size of the superconducting regions $d < \Lambda_Q$ at this temperature.

At this temperature, the superconducting regions will first grow near the nodes, as first pointed out by Fink and Grünfeld. Using nonlinear Ginzburg-Landau equations, they found that the superconducting order parameter has larger magnitude at the nodes than in the middle of the wire, which implies that superconductivity occurs at the nodes first as temperature is lowered.²³

As temperature is lowered further, the superconducting regions will grow in size from the nodes toward segments A and E instead of B and D, repectively, as shown in Fig. 7a. Such anisotropy is due to the following reasons. First, segments B and D have relative smaller cross section than A and E (Fig. 1), indicating that the current densities in B and D are higher than in A and E in realistic resistance measurements; Second, AFM image of surface roughness of the ring (Fig. 8) indicate segment B

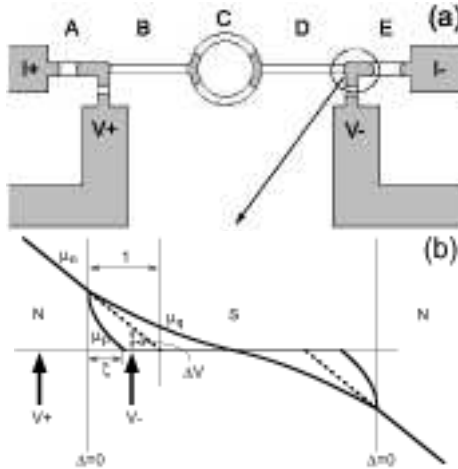


FIG. 7: a) Distribution of superconducting regions (gray areas) related to HTRP; b) Schematic of various potentials when the size of the superconducting region is smaller than Λ_Q at this temperature. The quantities shown are the same as those in Fig. 6.

and D are more disordered due to their larger height variations. Local T_c 's for segment B and D might be slightly lower than those for segment A and E.

For a superconducting region with its size $d < \Lambda_Q$, not all quasiparticles will convert to Cooper pairs and reach an equilibrium distribution, before the Cooper pairs that form in the superconducting region have to convert back to quasiparticles. At this temperature, since $d < \Lambda_Q$ for the superconducting regions (Fig. 7a), the ongoing charge imbalance process is distorted from the conventional one described above, where the superconducting region size, d , is at least larger than Λ_Q . While no calculation on the spatial distribution of μ_q and μ_p has been carried out in this sample configuration, we expect a distribution as illustrated schematically in Fig. 7b. If the a superconducting voltage lead is placed in region 1, excessive resistance, or a resistance anomaly, is expected, as observed experimentally.

At further lower temperatures, neighboring superconducting regions with $d < \Lambda_Q$ merge together to form larger superconducting islands with $d > \Lambda_Q$ (Fig. 9). However, phase slip centers will form at the weakest spots of segments B and D since they are the most disordered parts of the structure (Fig. 8) and carry the highest current density in the structure. The associated charge imbalance process is similar to that depicted schematically in Fig. 6.

D. Discussions

The two-stage charge imbalance model can explain the existence of two resistance peaks. It is clear from the discussion above that LTRP should be higher than HTRP. LTRP is mainly determined by the charge imbalance

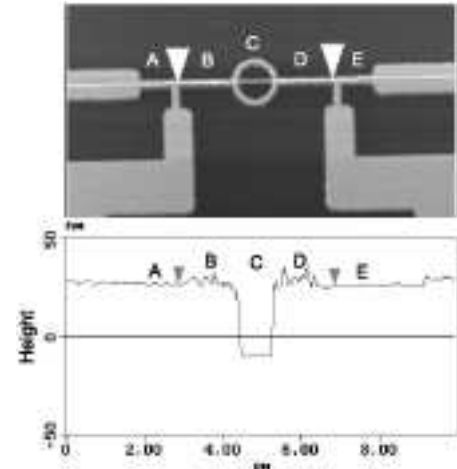


FIG. 8: Surface roughness of the $\text{Au}_{0.7}\text{In}_{0.3}$ rings. a) is the AFM image showing the selected scan line; b) is the height profile along the scan line shown in a).

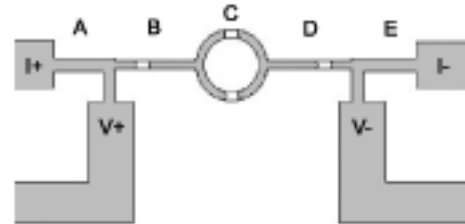


FIG. 9: Schematic of the superconducting islands (gray areas) at the temperatures where LTRP was observed. The size of the superconducting islands is larger than Λ_Q .

length Λ_Q , while HTRP is limited by the size of superconducting regions $d (< \Lambda_Q)$.

There is a relative decrease in resistance between the two resistance peaks (Fig. 2). Such a decrease is associated with the initial growth of superconducting regions toward segments B and D, respectively, right after HTRP is observed while temperature is lowered. The initial growth moves the N-S interfaces slightly away from the voltage leads while the overall size of the superconducting regions does not increase significantly. As shown in Fig. 7b, ΔV , proportional to the resistance anomaly, decreases as the voltage leads moves away from the interface, consistent with the experimental observations.

A rigorous comparison between the experimental data and the theoretical prediction, however, would require a microscopic theory that can describe the spatial variation of the quasiparticle potential μ_q over a length scale shorter than the usual charge imbalance length Λ_Q . Even for the LTRP which is related to the conventional charge imbalance process, Eq. 2 appears to overestimate its magnitude, similar to what was encountered in the previous work on Al structures¹⁴. In deriving this equation, complications due to disorder in the mesoscopic structures are not taken into account. Further theoretical analysis

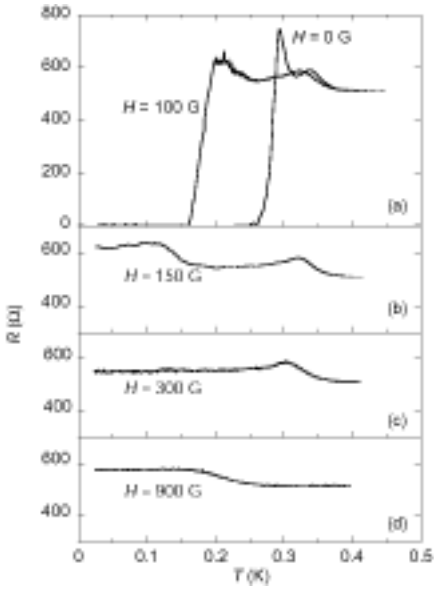


FIG. 10: $R(T)$ at several magnetic fields for Ring 6-100. The fields were applied perpendicular to the plane of the ring. A resistance plateau higher than R_N is shown down to the lowest temperature available ($< 20\text{mK}$).

is needed in order to account for our experimental results more quantitatively.

V. LOW-TEMPERATURE METALLIC STATE

Resistance anomaly in Al structures was found to be sensitive to magnetic field. Small field can suppress the anomaly significantly¹⁰. The effect of a magnetic field on the double resistance anomalies is illustrated in Fig. 10. The magnetic field was applied perpendicular to the plane of the ring. It is seen that while the LTRP was significantly suppressed in low field ($< 100\text{G}$), no significant change was found in the HTRP up to 300G .

Such a behavior can be understood in the two-stage charge imbalance model. LTRP is determined by Λ_Q but HTRP is determined by the size d of superconducting regions in the sample. A rapid suppression of τ_Q and Λ_Q in small magnetic field related to Eq. 7, as also shown in Ref. 14, can lead to the disappearance of LTRP while HTRP is not much affected.

An interesting feature emerging from Fig. 10 is the excessive resistance in zero temperature limit. At higher field $\sim 900\text{G}$, the resistance became independent of temperature down to the lowest temperature (20mK). However, the resistance value was larger than that of the normal state R_N . Therefore, the observed low-temperature resistance plateau may be called excessive resistance.

Recent experiment on $\text{Au}_{0.7}\text{In}_{0.3}$ films in parallel field

had revealed the similar feature⁷. However, in that case the low-temperature metallic state has a resistance less than R_N . Tunneling experiment showed that the film was composed of superconducting grains that are not Josephson coupled. Due to strong quantum phase⁸ and/or amplitude⁹ fluctuations, the superconducting grains remained uncoupled even in the zero temperature limit. An estimate of the grain size and concentration suggests that amplitude fluctuation play an essential role in the formation of this normal state.

Our observation of the excessive resistance down to the zero temperature limit in $\text{Au}_{0.7}\text{In}_{0.3}$ rings provides support for the existence of the metallic state in SNS junction arrays, even though in this case the array is 1D. We observed an excessive resistance because of charge imbalance. Although an accurate estimate of the size of the superconducting region d in this metallic state requires a rigorous microscopy theory which is unavailable, we can pursue in analogy to Eq. 2 to estimate its lower limit. To do this, we replace Λ_Q by $d/2$ in Eq. 2. We assume that two superconducting regions near the two voltage leads contributed to the resistance anomaly, ignoring other superconducting regions in between the two voltage leads that could lower the total resistance. With $x = 0$, we have $\Delta R = \rho d$. Comparing to the resistance plateau at 900G in Fig. 10 (a 10% rise above the normal-state R_N), the size of the superconducting region $\geq 0.4\mu\text{m}$, which is quite reasonable.

1D SNS junction arrays could be a potentially more interesting system to study the quantum superconductor-normal metal transition (SNT) than in 2D samples. Recently, it's argued that a SNT in $D = n$ dimension can be mapped into a $(n + z)$ dimensional classical phase transition, where z is the dynamical exponent which is 2 for 1D SNS arrays.²⁷ As any phase transition in dimension ≥ 4 is dominated by the mean field behavior, 1D SNT, with its corresponding classical phase transition in 3D, would be a preferred system to study quantum SNT dominated by critical fluctuations.

VI. CONCLUSION

In summary, we have observed $h/2e$ oscillations, double resistance anomalies, a magnetic-field-tuned metallic state with excessive resistance down to the zero temperature limit in 1D mesoscopic $\text{Au}_{0.7}\text{In}_{0.3}$ rings. A two-stage charge imbalance model based on the SNS structure and detailed geometry of the rings is proposed. We show that this model can explain our observations qualitatively. We would like to acknowledge useful discussions with Dr. B. Pannetier. This work is supported by NSF under grant DMR-0202534.

¹ Yu. Zadorozhny and Y. Liu, Phys. Rev. B **66**, 054512 (2002).

² Yu. Zadorozhny, D. R. Herman, and Y. Liu, Phys. Rev. B **63**, 144521 (2001).

³ Yu. Zadorozhny and Y. Liu, Europhys. Lett. **55**, 712 (2001).

⁴ F. Zhou and C. Biagini, Phys. Rev. Lett. **81**, 4724 (1998).

⁵ D. Das and S. Doniach, Phys. Rev. B **64**, 134511 (2001); D. Dalidovich and P. Phillips, Phys. Rev. Lett. **89**, 027001 (2002).

⁶ A. Kapitulnik, N. Mason, S. A. Kivelson, and S. Chakravarty, Phys. Rev. B **63**, 125322 (2001).

⁷ M. M. Rosario, to be published.

⁸ M. V. Feigel'man, A. I. Larkin, and M. A. Skvortsov, Phys. Rev. Lett. **86**, 1869 (2001).

⁹ B. Spivak, A. Zyuzin, and M. Hruska, Phys. Rev. B **64**, 132502 (2001).

¹⁰ P. Santhanam, C. C. Chi, S. J. Wind, M. J. Brady and J. J. Buchignano, Phys. Rev. Lett. **66**, 2254 (1991).

¹¹ V. V. Moshchalkov, L. Gielen, G. Neuttiens, C. Van Haesendonck, and Y. Bruynseraede, Phys. Rev. B **49**, R15412 (1994).

¹² I. L. Landau and L. Rinderer, Phys. Rev. B **56**, 6348 (1997).

¹³ M. Park, M. S. Isaacson and J. M. Parpia, Phys. Rev. B **55**, 9067 (1997).

¹⁴ C. Strunk, V. Bruyndoncx, C. Van Haesendonck, V. V. Moshchalkov, Y. Bruynseraede, C.-J. Chien, B. Burk, and V. Chandrasekhar, Phys. Rev. B **57**, 10854 (1998).

¹⁵ K. Yu. Arutyunov, D. A. Presnov, S. V. Lotkhov, and A. B. Pavolotski and L. Rinderer, Phys. Rev. B **59**, 6487 (1999).

¹⁶ C.-J. Chien and V. Chandrasekhar, Phys. Rev. B **60**, 3655 (1999).

¹⁷ Yu. D. Sharvin and Yu. V. Sharvin, JETP Lett. **34**, 272 (1981).

¹⁸ G. J. Dolan and L. D. Jackel, Phys. Rev. Lett. **39**, 1628 (1977).

¹⁹ J. R. Waldrum, Proc. R. Soc. London, Ser. A **345**, 231 (1975).

²⁰ B. I. Ivlev and N. B. Kopnin, Adv. Phys. **33**, 47 (1984).

²¹ Fei Zhou, Int. J. Mod. Phys. B **13**, 2229 (1999).

²² V. V. Schmidt, The Physics of Superconductors.

²³ H. J. Fink and V. Grunfeld, Phys. Rev. B **31**, 600 (1985).

²⁴ A. Schmid and G. Schön, J. Low Temp. Phys. **20**, 207 (1975).

²⁵ A. M. Kadin, W. J. Skocpol, and M. Tinkham, J. Low Temp. Phys. **33**, 481 (1978).

²⁶ H. Courtois, Ph. Gandit, D. Mailly, and B. Pannetier, Phys. Rev. Lett. **76**, 130 (1996).

²⁷ Subir Sachdev, Philipp Werner, and Matthias Troyer, Phys. Rev. Lett. **92**, 237003 (2004).